Weight Loss–Associated Induction of Peroxisome Proliferator–Activated Receptor-α and Peroxisome Proliferator–Activated Receptor-γ Correlate With Reduced Atherosclerosis and Improved Cardiovascular Function in Obese Insulin-Resistant Mice

Wim Verreth, MECGB; Dieuwke De Keyzer, MECGB; Michel Pelat, PhD; Peter Verhamme, MD, PhD; Javier Ganame; John K. Bielicki, PhD; Ann Mertens, PhD, MD; Rozenn Quarck, PhD; Nora Benhabilès, PhD; Gérard Marguerie, PhD; Bharti Mackness, PhD; Mike Mackness, PhD; Ewa Ninio, PhD; Marie-Christine Herregods, PhD, MD; Jean-Luc Balligand, PhD, MD; Paul Holvoet, PhD

Background—Weight loss in obese insulin-resistant but not in insulin-sensitive persons reduces coronary heart disease risk. To what extent changes in gene expression are related to atherosclerosis and cardiovascular function is unknown.

Methods and Results—We studied the effect of diet restriction–induced weight loss on gene expression in the adipose tissue, the heart, and the aortic arch and on atherosclerosis and cardiovascular function in mice with combined leptin and LDL-receptor deficiency. Obesity, hypertriglyceridemia, and insulin resistance are associated with hypertension, impaired left ventricular function, and accelerated atherosclerosis in those mice. Compared with lean mice, peroxisome proliferator–activated receptors (PPAR)-α and PPAR-γ expression was downregulated in obese double-knockout mice. Diet restriction caused a 45% weight loss, an upregulation of PPAR-α and PPAR-γ, and a change in the expression of genes regulating glucose transport and insulin sensitivity, lipid metabolism, oxidative stress, and inflammation, most of which are under the transcriptional control of these PPARs. Changes in gene expression were associated with increased insulin sensitivity, decreased hypertriglyceridemia, reduced mean 24-hour blood pressure and heart rate, restored circadian variations of blood pressure and heart rate, increased ejection fraction, and reduced atherosclerosis. PPAR-α and PPAR-γ expression was inversely related to plaque volume and to oxidized LDL content in the plaques.

Conclusions—Induction of PPAR-α and PPAR-γ in adipose tissue, heart, and aortic arch is a key mechanism for reducing atherosclerosis and improving cardiovascular function resulting from weight loss. Improved lipid metabolism and insulin signaling is associated with decreased tissue deposition of oxidized LDL that increases cardiovascular risk in persons with the metabolic syndrome. **(*Circulation*. 2004;110:3259-3269.)**

Key Words: atherosclerosis ■ circadian rhythm ■ genes ■ lipoproteins ■ obesity

Insulin resistance is now receiving increasing attention not only as a precursor to type 2 diabetes but also as a predictor of increased risk of cardiovascular disease.[1] Fat distributed in the abdominal region is a risk factor for type 2 diabetes and cardiovascular disease and is associated closely with insulin resistance.[2] Weight loss in insulin-resistant but not in insulin-sensitive obese persons reduces their risk of coronary heart disease (CHD).[3] It is not known, however, to what extent changes in the intra-abdominal adipose gene expression profile are important for the reduction of the risk.[4]

Several adipokines, and more specifically peroxisome proliferator–activated receptors (PPARs), regulate a number of the processes that contribute to the development of atherosclerosis, including dyslipidemia, arterial hypertension, endothelial dysfunction, insulin resistance, and vascular remodeling. Adipokines are preferentially expressed in intra-abdominal adipose tissue, and the secretion of proinflammatory adipokines is elevated with increasing adiposity. Approaches to reduce adipose tissue depots, including diet restriction, could stimulate adipocyte differentiation and as a

Received June 24, 2004; revision received July 28, 2004; accepted August 3, 2004.

From the Cardiovascular Research Unit of the Center for Experimental Surgery and Anesthesiology (W.V., D.D.K., P.V., A.M., R.Q., P.H.), Department of Cardiology (J.G., M.-C.H.), Katholieke Universiteit Leuven, and the Department of Medicine, Unit of Pharmacology and Therapeutics, Université Catholique de Louvain (M.P., J.-L.B.), Belgium; Lawrence Berkeley National Laboratory, Berkeley, Calif (J.K.B.); the University of Manchester, Department of Medicine, Manchester Royal Infirmary, Manchester, UK (B.M., M.M.); and Clinigenetics, Nimes (N.B., G.M.), and INSERM U525, Institut Fédératif CMV, Université Pierre et Marie Curie, Paris (E.N.), France.

Correspondence to Paul Holvoet, PhD, Center for Experimental Surgery and Anesthesiology, Katholieke Universiteit Leuven, Herestraat 49, B-3000 Leuven, Belgium. E-mail paul.holvoet@med.kuleuven.ac.be

Circulation **is available at http://www.circulationaha.org** **DOI: 10.1161/01.CIR.0000147614.85888.7A**

result positively alter adipokine levels, thereby reducing the severity of their resulting diseases.

Mice with combined leptin and LDL-receptor deficiency (DKO) feature obesity, dyslipidemia, hypertension, insulin resistance, and impaired glucose tolerance and/or diabetes. These metabolic syndrome attributes are associated with increased oxidative stress and accelerated atherosclerosis.[5] Therefore, we chose these mice to study the effect of weight loss on metabolic syndrome attributes, atherosclerosis, and cardiovascular function. Because weight loss in DKO mice was associated with a reduction in markers of cardiovascular risk, our second objective was to identify the underlying mechanisms. Therefore, we studied the effect of weight loss on changes in the gene expression profiles in the visceral adipose tissue that correlate with changes in lipoprotein and lipid profile, oxidative stress, insulin sensitivity, glucose tolerance, blood pressure (BP) and heart rate (HR) regulation, and atherosclerosis. We show here that PPAR-α and PPAR-γ expression in adipose tissue is downregulated in DKO mice compared with lean LDLR$^{(-/-)}$ mice and that weight loss results in restoring PPAR expression. PPAR expression was also restored in the aortic arch and the heart tissue.

Methods

Experimental Protocol

Homozygous LDL-receptor–knockout mice (LDLR$^{(-/-)}$), heterozygous ob/+, and C57BL6 mice were purchased from Jackson Laboratory, Bar Harbor, Me. LDLR$^{(-/-)}$ mice were backcrossed into a C57BL6 background to the 10th generation. To obtain DKO mice with combined leptin deficiency (ob/ob) and LDL-receptor deficiency, LDLR$^{(-/-)}$ and ob/+ mice were crossed as previously described.[5] All offspring were genotyped by polymerase chain reaction (PCR) techniques.[6] All mice were housed at 22°C on a fixed 12/12-hour light/dark cycle. Experimental procedures in animals were performed in accordance with protocols approved by the Institutional Animal Care and Research Advisory Committee.

All mice were fed standard chow containing 4% fat (Pavan Service). Food intake of free-fed DKO mice was ≈5.7 g/d from weaning for 12, 24, or 36 weeks. Since our previous study,[5] animal fat has been replaced with vegetable oils in the standard chow, resulting in lower cholesterol levels. Food intake of diet-restricted mice was restricted to 2.5 g/d for 12 weeks between 12 and 24 weeks of age (24-week diet-restricted mice) or between 24 and 36 weeks of age (36-week diet-restricted mice) (Figure 1). This amount corresponds to the daily intake of lean LDLR$^{(-/-)}$ mice.

Body Composition

Body composition was measured with PIXImus Mouse Densitometry (Lunar Corp).[7]

Real-Time RT-PCR and Microarray Analysis

The level of mRNA expression for PPAR-α and PPAR-γ in white visceral (intra-abdominal) adipose tissue from C57BL6, LDLR$^{(-/-)}$, and Ob/Ob mice at 24 weeks; in free-fed DKO mice at 12, 24, and 36 weeks; and in 24-week and 36-week diet-restricted DKO mice was measured by real-time reverse transcription (RT)-PCR. Total RNA was extracted from mouse visceral adipose tissue with the Trizol reagent (InVitrogen) and purified on an RNeasy kit column (Qiagen). First-strand cDNA was generated from total RNA by RT using random primers from Takara and Superscript III reverse transcriptase (InVitrogen). Quantitative real-time PCR was performed using SybrGreen master mix according to the supplier protocols (Applied Biosystems). Oligonucleotides (InVitrogen) used as forward primer (F) and reverse primer (R) were: for mouse PPAR-α, F: 5′-TCAGGGTACCACTACGGAGTTCA-3′; R: 5′-CCGAATAGTTCGCCGAAAGA-3′; for mouse PPAR-γ, F: 5′-GCAGCTACTGCATGTGATCAAGA-3′; R: 5′-GTCAGCGGGTGGGACTTTC-3′; and for mouse β-actin, F: 5′-ACGGCCAGGTCATCACTATTG-3′; R: 5′-CACAGGATTCCATACCCAAGAAG-3′. The level of mRNA expression for PPAR-α and PPAR-γ was calculated using the threshold cycle (C_t) value, ie, the number of PCR cycles at which the fluorescent signal during the PCR reaches a fixed threshold. For each sample, the C_t both for the gene of interest and for the housekeeping gene β-actin were determined to calculate $\Delta C_{t,sample}$ ($C_{t,target\ gene} - C_{t,housekeeping\ gene}$), thus normalizing the data and correcting for differences in amount and/or quality between the different RNA samples. The expression levels were related to an external calibrator consisting of intra-abdominal adipose tissue from C57BL6 control mice. Subsequently, $\Delta\Delta C_t$ ($\Delta C_{t,sample} - \Delta C_{t,calibrator}$) was determined, and the relative expression levels were calculated from $2^{-\Delta\Delta Ct}$ according to the manufacturer's instructions (Applied Biosystems). mRNA expression levels are thus indicated as arbitrary units ±SD.[8]

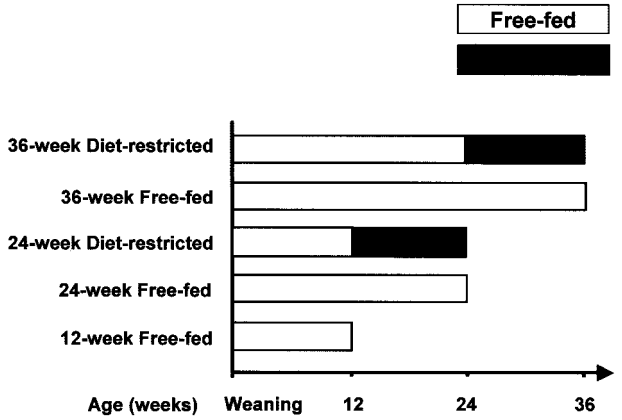

Figure 1. Experimental protocol. All mice were fed standard chow containing 4% fat. Food intake of free-fed DKO mice was ≈5.7 g/d. Food intake was restricted to 2.5 g/d (black box) for 12 weeks between 12 and 24 weeks (24-week diet-restricted mice) or between 24 and 36 weeks (36-week diet-restricted mice).

Because we observed upregulation of PPAR-α and PPAR-γ in the adipose tissue from diet-restricted compared with free-fed DKO mice, we also compared PPAR expression in extracts from the heart and the aortic arch of those mice.

To identify genes that change according to the differences in PPAR expression, we performed 3 independent experiments with Agilent Mouse cDNA microarrays (product No. G4104A) that contain 9600 clones; among them, 8737 are unique and have a GenBank ID number. The source contents come from Incyte Mouse Unigene1, and the cDNA probe length lies between 500 and 1000 bp. We compared the abundance of transcripts in 2 mRNA samples, 1 from the visceral adipose tissue from a free-fed mouse, the other from a diet-restricted mouse, both at 24 weeks. The sample preparation consisted of 2 rounds of amplification from total RNA for dye swap hybridization. We used the cDNA labeling protocol recommended by Agilent (G2557 A kit), with the following modifications: 2.5 μg random hexamer primers (Invitrogen) at 3 μg/μL were added, and 4 μg RNA for each microarray chip was used. The hybridization protocol recommended by Agilent was used according to kit G4104A. Slides were imaged with an Agilent scanner (Agilent G2565AA) with a resolution of 5 μm. Spot addressing, grid positioning, segmentation, and intensity extraction (signal and background) were performed with Agilent Feature Extractor V.5.1.1 software (Agilent G2566AA Feature Extraction Software). Each spot was flagged according to 11 quality measures. In the general configuration, "Spot Finder," "PolyOutlierFlagger," and "CoolieCutter" were retained. In Find Spot configuration, "Autofind corners" was selected, with a "Dev Limit" of 70 μm. In CoolieCutter configuration, "Reject based on IQR" of 1.42 for feature and

background was selected. In the PolyOutlierFlagger configuration, "Non-Uniformity Outlier Flagging" and "Population Outlier Flagging" were selected with the default. To correct print tip– and intensity-dependent effects, raw data were normalized in Clinigenetics according to a composite method based on dye swap, print tip, and scale normalization algorithms.[9]

We also performed 2 experiments with Agilent mouse 60-mer microarrays to compare the expression of selected genes in free-fed and diet-restricted mice at 24 weeks. More detailed microarray specifications can be downloaded from www.chem.agilent.com.

Biochemical Analyses

Blood of conscious mice was collected by tail bleeding into EDTA tubes after an overnight fast. Plasma was obtained by centrifugation, and lipoproteins were separated by fast protein liquid chromatography.[10] Protein levels were determined according to Bradford, cholesterol by high-performance liquid chromatography,[11] triglycerides with a diagnostic reagent kit (Sigma-Aldrich), glucose with a glucometer (Menarini Diagnostics), plasma insulin with a mouse insulin ELISA (Mercodia), and adiponectin with a mouse adiponectin ELISA (Bio-Cat). Insulin resistance was calculated by a homeostasis model assessment (HOMA)=fasting serum insulin (mU/L) times fasting blood glucose (mmol/L)/22.5. To determine glucose tolerance, glucose was measured in samples obtained by tail bleeding before and 15, 30, 60, 120, and 240 minutes after intraperitoneal glucose administration (20% glucose solution; 2 g/kg).[12]

Paraoxonase (PON), PAF-acetylhydrolase (AH), and lecithin:cholesterol acyltransferase (LCAT) activities were measured as previously described.[13–15] The titers of Ig autoantibodies against oxidized LDL were determined in individual plasma samples (1:500 dilution). The amount of Ig bound to the oxidized LDL antigen was detected with alkaline phosphatase–labeled anti-mouse IgG. Data are expressed as relative absorbance units.[5]

Atherosclerosis

The extent of atherosclerosis was determined by analysis of cross sections from the aortic root. Approximately ten 7-μm frozen sections per staining per animal were used for morphometric and immunohistochemical analysis. Lipids were stained with oil red O, oxidized LDL (ox-LDL) with mAb4E6, smooth muscle cells with an α-actin specific antibody (Dako), and macrophages with an antibody against mouse Mac-3 antigen (Pharmingen). Blinded analysis of positive immunostained sections was performed with the Quantimet600 image analyzer (Leica).[5]

Telemetry

BP signals and HR derived from pressure waves from the aortic arch were measured in conscious, unrestrained animals with surgically implanted miniaturized telemetry devices (DSI model TA11-PA-C20, Datascience Corp). These devices, allowing continuous recordings of BP and HR for several weeks, were surgically installed under general anesthesia, as described previously,[16] at the age of 24 weeks. After 1 week of recovery, short-term (300 seconds) or long-term (24 hours) recordings were acquired online in conscious, freely moving mice, and digitized data (sampling rate, 2000 Hz) were collected using HEM 3.4 software (Notocord systems).

Circadian Variation of BP and HR

BP and HR were recorded continuously for 24 hours. Mean values of BP and HR were calculated for each 60-minute sequence of recording. Averages were also calculated for light and dark periods.

Spectral Analysis of HR and BP Variability

Spectral analysis using a fast Fourier transformation algorithm on sequences of 512 points was performed with HEM 3.4 software on BP and HR recordings. The area under the curve was calculated for the very-low-frequency (VLF, 0.05 to 0.4 Hz), low-frequency (LF, 0.4 to 1.5 Hz), and high-frequency (HF, 1.5 to 5.0 Hz) bands as previously defined in the mouse.[17–19] Spectral variability at each bandwidth was normalized to the total spectral area.

Echocardiography

Transthoracic echocardiography of C57BL6, 24-week free-fed, and 24-week diet-restricted mice was performed with the use of a Philips SONOS 5500 with a 5- to 12-MHz S12 neonatal ultraband cardiac phased probe.[20] Mice were anesthetized with pentobarbital and put on a heating pad to maintain body temperature. HR was measured in M-mode. The fractional area change, a measure for the ejection fraction (EF), was calculated from the left ventricular (LV) cross-sectional area (2D short axis) by use of the equation EF (%)=[(LVDA−LVSA)/LVDA]×100, where LVDA is the LV diastolic area and LVSA is the LV systolic area.

Statistical Analysis

Groups were compared by the Kruskal-Wallis test (Graph Pad Prism version 3.02) followed by Dunn's multiple-comparisons test. Correlations were calculated by use of the nonparametric Spearman correlation coefficient. A probability value of $P<0.05$ was considered statistically significant.

Results

Weight and Fat Mass

Figure 2A shows a 45% weight loss of 24-week diet-restricted mice compared with free-fed mice of the same age. Similar changes were observed in 36-week diet-restricted mice (Figure 2A). The reduction of weight was because of a 33% loss of fat mass (Figure 2B).

PPAR Gene Expression

PPAR-γ and PPAR-α gene expression in white visceral adipose tissue was measured with RT-PCR. In DKO mice, PPAR-γ and PPAR-α expression decreased with time (Figure 3A). At 24 weeks, PPAR-γ expression was lower in DKO mice compared with $LDLR^{(-/-)}$ and Ob/Ob mice, and PPAR-α expression was lower in DKO and Ob/Ob mice compared with $LDLR^{(-/-)}$ (Figure 3B). Compared with free-fed DKO mice at 24 weeks, the expression of PPAR-γ was 1.7-fold higher, and that of PPAR-α was 1.9-fold higher, in the 24-week diet-restricted group. Compared with free-fed DKO mice at 36 weeks, the expression of PPAR-γ was also 1.7-fold higher, and that of PPAR-α was 3.2-fold higher, in the 36-week diet-restricted group (Figure 3C).

PPAR-α and PPAR-γ expression (in arbitrary units) was higher in the hearts of diet-restricted mice compared with free-fed DKO mice: 1.4 ± 0.2 versus 0.9 ± 0.2 and 1.3 ± 0.2 versus 0.8 ± 0.1, respectively ($n=6$ each; $P<0.01$ each). PPAR-α and PPAR-γ expression was also higher in the aortic arch of diet-restricted mice: 1.2 ± 0.5 versus 0.4 ± 0.1 and 0.7 ± 0.2 versus 0.4 ± 0.1, respectively ($P<0.01$ each).

Microarray Analysis of Gene Expression in Adipose Tissue

We used microarray to identify genes of which the expression in the visceral adipose tissue changes according to the changes we saw in PPAR expression. On cDNA chips (Agilent), 222 genes were significantly upregulated (mean ratio, >1.5) in the adipose tissue of 24-week diet-restricted mice and 114 genes were downregulated (ratio, <0.5) compared with 24-week free-fed mice. Table 1 shows the upregulated and downregulated genes that are associated with

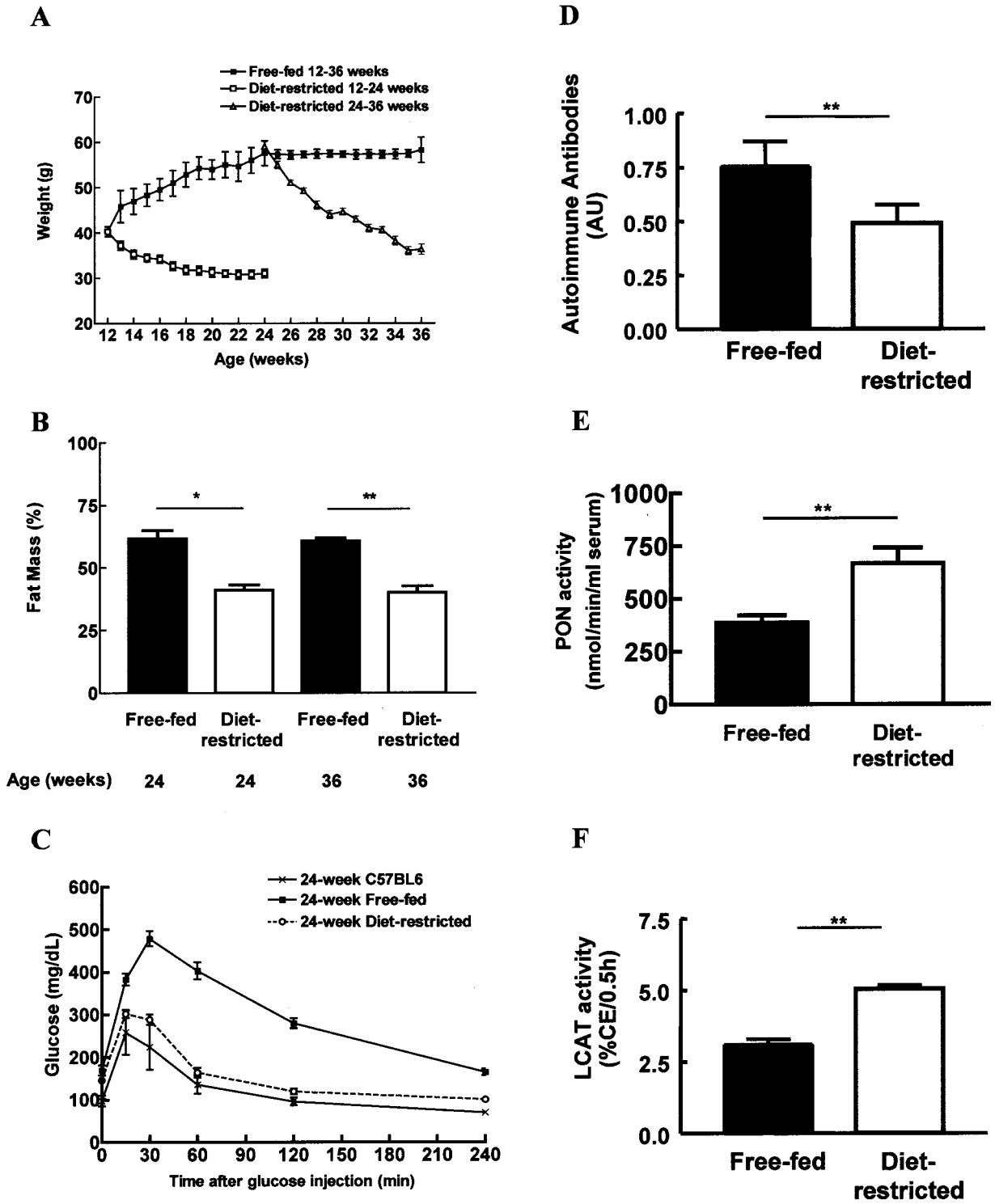

Figure 2. A, Weight loss in 24-week diet-restricted (n=20) and 36-week diet-restricted (n=11) DKO mice; B, fat mass in free-fed (n=9 per group) and diet-restricted (n=8 per group) DKO mice; C, glucose tolerance in C57BL6 (n=6), 24-week free-fed (n=16), and 24-week diet-restricted (n=16) DKO mice; effect of diet restriction on titer of Ig antibodies against oxidized LDL (D) and on PON (E) and LCAT (F) activity. *$P<0.05$; **$P<0.01$.

adipocyte differentiation, glucose transport and insulin sensitivity, hypertriglyceridemia, oxidative stress, and inflammation. There was a trend toward lower tumor necrosis factor-α expression (ratio, 0.60±0.13).

On Agilent mouse 60-mer microarray slides, the mean relative ratios (for 2 independent experiments) were 2.4 for PPAR-α, 3.1 for PPAR-γ, 4.9 for Ras, 2.7 for C/EBPα, 2.6 for FABP, 2.0 for angiotensinogen, 2.4 for LPL, 3.3 for

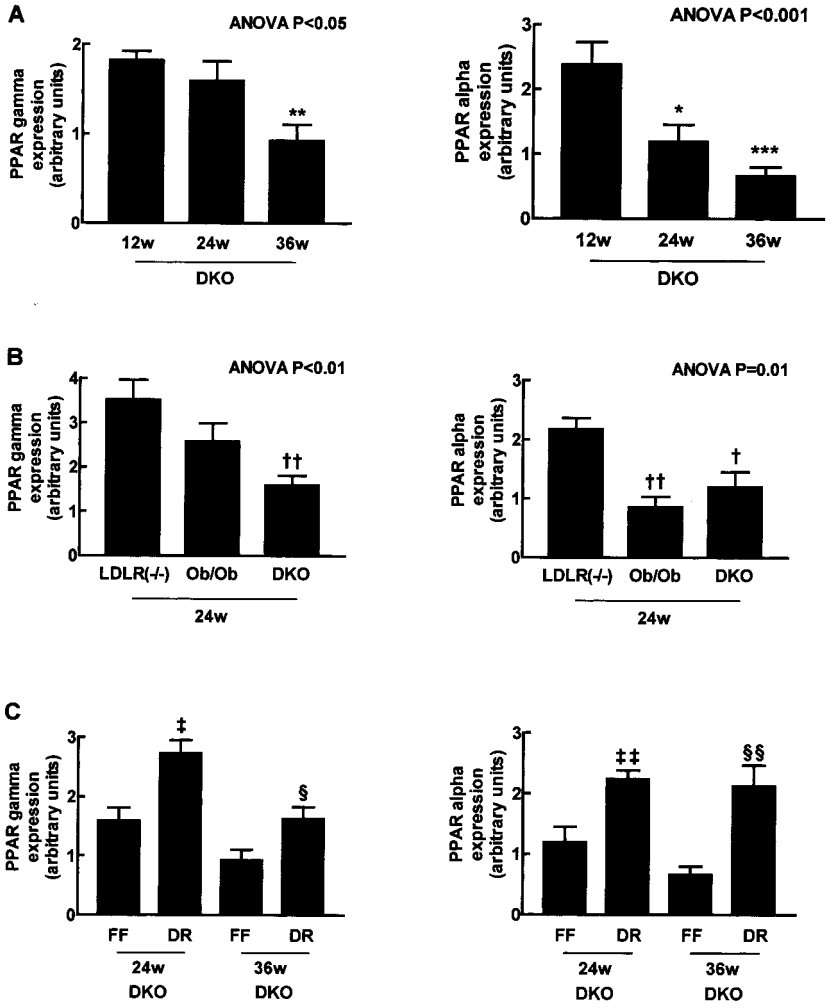

Figure 3. A, PPAR-γ and PPAR-α expression in intra-abdominal adipose tissue from 12-week (n=8), 24-week (n=5), and 36-week (n=8) free-fed DKO mice. B, PPAR-γ and PPAR-α expression in lean LDLR$^{(-/-)}$ (n=8), Ob/Ob (n=6), and DKO obese (n=5) mice at 24 weeks. C, Effect of diet restriction on PPAR-γ and PPAR-α expression at 24 (free-fed, n=5; diet-restricted, n=7) and 36 (n=8 per group) weeks. FF, free-fed, DR, diet-restricted; *P<0.05, **P<0.01, and ***P<0.001 vs 12-week DKO mice; †P<0.05 and ††P<0.01 vs LDLR$^{(-/-)}$ mice; ‡P<0.05 and ‡‡P<0.01 vs 24-week free-fed DKO mice; §P<0.05 and §§P<0.01 vs 36-week free-fed DKO mice.

VLDL receptor, 2.7 for hormone sensitive lipase, 2.7 for superoxide dismutase-3, 2.5 for glutathione peroxidase, and 4.6 for nitric oxide synthase (NOS)-3.

Blood Analysis

Table 2 shows baseline blood parameters. Weight loss resulted in a 72% decrease of triglycerides in the 24-week diet-restricted group without changing total, non-HDL, and HDL cholesterol levels. Results in 36-week diet-restricted mice were comparable. Compared with free-fed DKO mice, insulin levels were lower in the diet-restricted groups but glucose levels were not. HOMA for diet-restricted mice was 77% lower than that for free-fed mice. HOMA for diet-restricted mice was still 20-fold higher than that of lean mice [C57BL6 and LDLR$^{(-/-)}$ mice]. Diet restriction resulted in a normalization of the glucose tolerance (Figure 2C). In the 24-week diet-restricted group, weight loss resulted in an increase of plasma adiponectin from 29±8.6 ng/mL (n=11) to 45±24 ng/mL (n=14; P<0.05).

Titer of Autoimmune Antibodies and PON, PAF-AH, and LCAT Activity

Weight loss was associated with a 1.5-fold decrease of the titer of Ig autoantibodies against oxidized LDL (Figure 2D), a 1.7-fold increase in PON activity (Figure 2E), and a 1.6-fold increase of the LCAT activity (Figure 2F). The total plasma PAF-AH activity was similar in free-fed and diet-restricted mice.

Atherosclerosis

Figure 4 shows representative oil red O–stained sections of the aortic root from free-fed mice at 12, 24, and 36 weeks and from diet-restricted mice at 24 and 36 weeks. Lesions in 12-week free-fed mice were very small fatty streaks. Plaque volumes increased from 0.005±0.003 mm^3 at 12 (n=8) to 0.166±0.036 mm^3 at 24 (n=10) and 0.302±0.101 mm^3 at 36 (n=8) weeks. Plaque volumes in 24-week diet-restricted mice were 12 times smaller than in 24-week free-fed mice (Figure 4). Plaque volumes in 36-week diet-restricted mice were similar to those in 24-week free-fed mice and 2.1 times smaller than in 36-week free-fed mice (Figure 4). Lipid content of plaques in 36-week diet-restricted mice was only marginally lower than in 36-week free-fed mice; macrophage content was 52% lower (9±3% versus 18±4%; P<0.01) and ox-LDL content was 16% lower (62±9% versus 73±5%; P<0.05), whereas smooth muscle content was 95% higher (25±7% versus 13±4%; P<0.05).

Triglycerides correlated with plaque volume (Spearman correlation coefficient, R_S=0.78; P<0.01). There was a

TABLE 1. Gene Expression in the Intra-Abdominal Adipose Tissue From Diet-Restricted Compared With Free-Fed DKO Mice at the Age of 24 Weeks

Probe Name	GenBank ID	Unigene ID	Name	Exp 1	Exp 2	Exp 3	Mean	SD
317536	W34083	Mm.3020	Peroxisome proliferator–activated receptor-γ	2.0	0.9	4.0	2.3	1.6
1366165	AI020897	Mm.3903	Ras, dexamethasone-induced 1	3.8	4.6	4.9	4.4	0.6
935273	AA617613	Mm.2411	Ras-GTPase activating protein	2.5	1.6	2.1	2.1	0.5
517625	AA066475	Mm.10661	Solute carrier family 2 (facilitated glucose transporter), member 4	2.7	1.9	5.9	3.5	2.1
540533	AA161908	Mm.34537	CCAAT/enhancer binding protein (C/EBP), α	1.5	2.0	3.7	2.4	1.1
523460	AA080270	Mm.582	Fatty acid binding protein 4, adipocyte	1.0	1.7	2.8	1.8	0.9
987842	AA571053	Mm.8854	Angiotensinogen	1.8	2.8	2.0	2.2	0.5
620940	AA177240	Mm.12837	Nitric oxide synthase 3, endothelial cell	1.6	1.2	4.6	2.5	1.9
313176	W10495	Mm.1373	Peroxisome proliferator activated receptor-α	1.5	1.6	2.4	1.9	0.5
1227378	AA739040	Mm.1514	Lipoprotein lipase	2.8	1.0	19	7.8	10
597754	AA154113	Mm.1721	Lipase, hormone sensitive	3.8	2.2	2.7	2.9	0.8
446084	AA020307	Mm.4141	VLDL receptor	1.3	1.2	4.5	2.3	1.9
1005832	AA606943	Mm.2400	Glutathione peroxidase 4	1.6	1.6	2.4	1.8	0.4
459497	AA027504	Mm.2407	Superoxide dismutase 3, extracellular	1.2	1.2	2.7	1.7	0.9
1383594	AI120986	Mm.23905	Platelet factor 4	0.3	0.2	0.6	0.4	0.2
1329349	AA930477	Mm.19844	Arachidonate 5-lipoxygenase activating protein	0.2	0.1	0.6	0.3	0.2
332372	W08586	Mm.28973	Intercellular adhesion molecule	0.4	0.5	0.5	0.5	0.1
1230835	AA880028	Mm.1708	CD22 antigen	0.5	0.5	0.2	0.4	0.2
642342	AA185112	Mm.200904	CD44 antigen	0.3	0.2	0.4	0.3	0.1
1020649	AA646061	Mm.2692	CD53 antigen	0.4	0.2	0.3	0.3	0.1
1263770	AA863715	Mm.15819	CD68 antigen	0.25	0.18	0.49	0.3	0.2
1381984	AA8332859	Mm.1252	Mast cell protease 5	0.08	0.09	0.16	0.1	0.04
314268	W10007	Mm.7409	Mast cell protease 6	0.16	0.2	0.31	0.2	0.08
1245329	AA821616	Mm.4054	Thromboxane A synthase-1, platelet	0.14	0.14	0.38	0.2	0.1

negative correlation between both PPAR-γ and PPAR-α expression and plaque volume (Figure 5A) and between both PPAR-γ and PPAR-α expression and percentage of the plaque surface that was stained for ox-LDL (Figure 5B) in free-fed and diet-restricted DKO mice. PPARs were not correlated with macrophage content, but macrophage content correlated with ox-LDL content (R_S=0.74; P<0.01).

BP, HR, and Ejection Fraction

In C57BL6 mice (n=5), continuous (24 hours) BP and HR recordings revealed a typical variation during the light-dark cycle, ie, light (corresponding to a resting period for mice) values of systolic (S) BP, diastolic (D) BP, and HR were significantly lower than dark (activity period for mice) values. By contrast, circadian variations of HR and BP were totally abolished in free-fed DKO mice (n=5) (Figure 6A). These mice also had higher mean 24-hour SBP (128±1.3 versus 112±1.3 mm Hg; P<0.05) and DBP values (93±1.1 versus 87±0.8 mm Hg; P<0.05) and higher mean HR compared with controls (544±5.5 versus 454±7.2 bpm; P<0.05). Diet restriction reduced all parameters in DKO mice to C57BL6 values (117.5±1.8 mm Hg, 87.8±1.3 mm Hg, and 402±6.9 bpm, respectively; n=5). Similar changes were observed during light and dark cycles (Figure 6A).

TABLE 2. Baseline Blood Parameters and Effect of Diet Restriction on Blood Parameters

	C57BL6	LDLR$^{(-/-)}$	Ob/Ob	24-Week Free-Fed DKO	24-Week Diet-Restricted DKO	36-Week Free-Fed DKO	36-Week Diet-Restricted DKO
Total cholesterol, mg/dL	78±19	213±68†	136±51*	537±276‡	446±200‡	422±154‡	550±183‡
Non-HDL cholesterol, mg/dL	37±18	156±52†	69±36	491±278‡	383±184‡	366±149‡	475±175‡
HDL cholesterol, mg/dL	41±20	57±35	67±18*	46±18	63±21	56±66	75±17*
Triglycerides, mg/dL	23±5	65±20†	29±7	596±293‡	130±6‡§	497±368‡	80±25‡¶
Glucose, mmol/L	4.3±0.83	4.6±0.49	10±2.8‡	12±3.1‡	9.2±5.3†	12±4.2‡	13±7.6†
Insulin, mU/L	130±100	110±78	3190±580‡	3190±1110‡	930±440‡‖	3400±1740‡	720±320‡#
HOMA	25±4	22±3	1417±254‡	1701±312‡	380±35‡‖	1813±325‡	416±42‡#

Data are mean±SD for 10–12 mice per group. *P<0.05, †P<0.01, ‡P<0.001 vs C57BL6; §P<0.05, ‖P<0.01 vs 24-week diet-restricted DKO; ¶P<0.05 and #P<0.01 vs 36-week diet-restricted DKO mice.

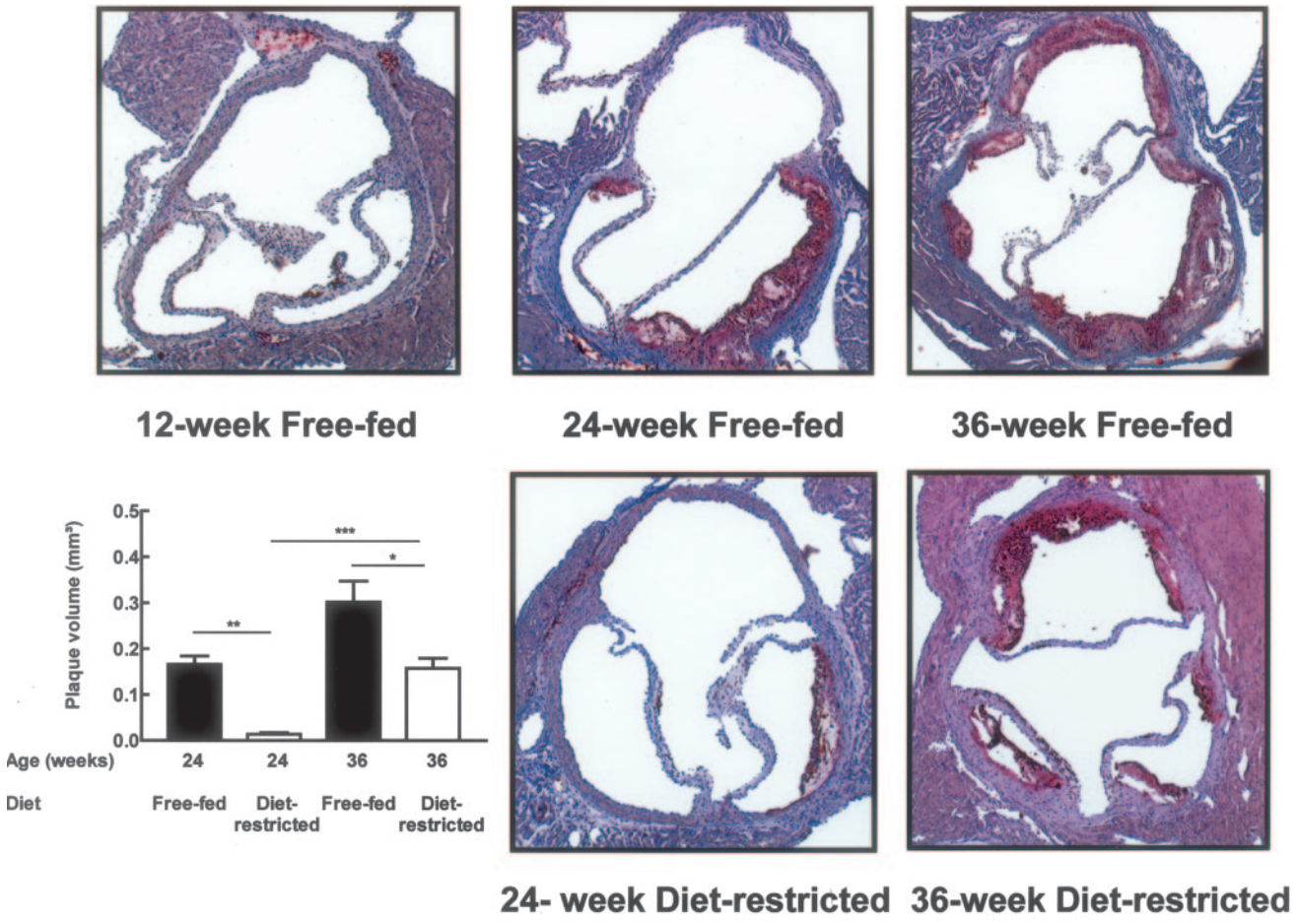

Figure 4. Representative cross sections of aortic arch from free-fed DKO mice at 12, 24, and 36 weeks and from 24-week and 36-week diet-restricted mice. Plaque volumes in aortic arch from 24- and 36-week free-fed (n=10 and n=8, respectively) and diet-restricted (n=10 for both) DKO mice. $^{*}P<0.05$; $^{**}P<0.01$; $^{***}P<0.001$.

Figure 6A shows that diet restriction also restored the circadian variations of SBP and HR in DKO mice. Analysis of BP and HR variability in DKO mice revealed an increased variability of SBP in the VLF domain (<0.4 Hz, reflecting neurohumoral, including NO, influences), an increased variability of SBP in the LF domain (0.4 to 1.5 Hz, reflecting adrenergic tone), and, conversely, a decreased variability of HR in the HF domain (>1.5 Hz, reflecting vagal control). All

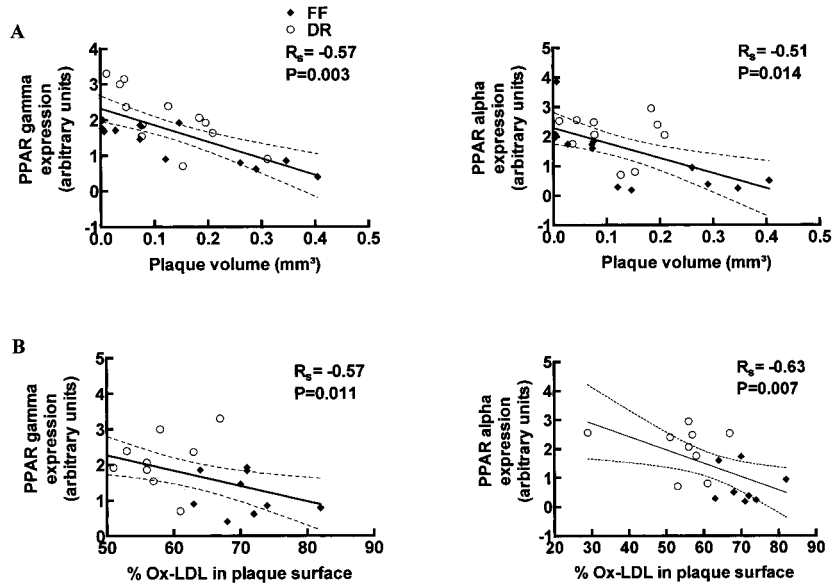

Figure 5. A, Correlation of PPAR-γ (n=25) and PPAR-α (n=23) expression with aortic plaque volume in free-fed (FF) and diet-restricted (DR) DKO mice. B, Correlation between both PPAR-γ (n=19) and PPAR-α (n=17) expression and ox-LDL in aortic plaques in free-fed and diet-restricted DKO mice.

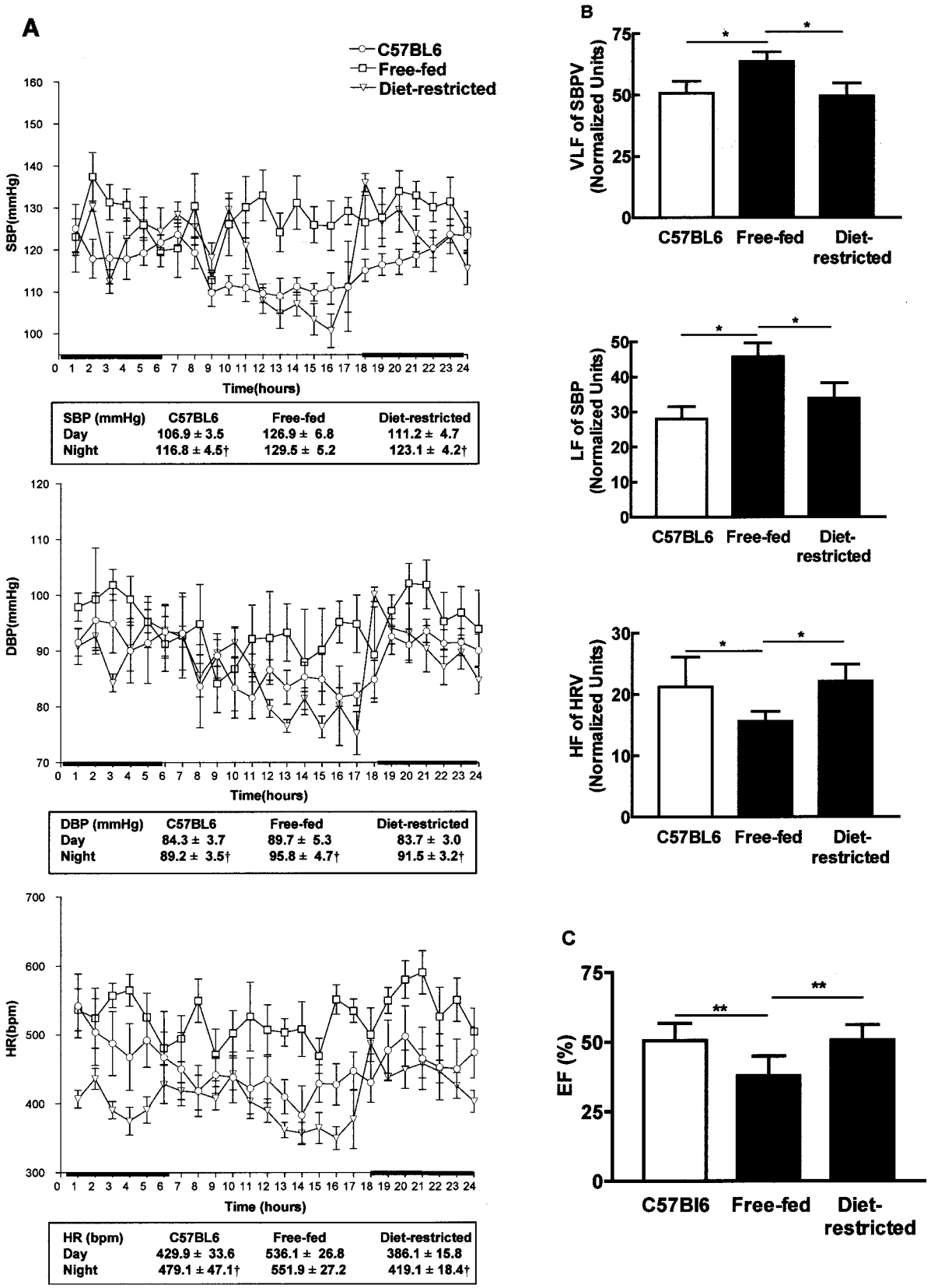

Figure 6. A, Circadian variations of SBP, DBP, and HR in C57BL6 control mice (n=5) and in free-fed (n=5) and diet-restricted (n=5) DKO mice at 24 weeks. Tables indicate mean day and night values. B, Variation of SBP at VLF and at LF and variation of HR at HF in C57BL6 control mice (n=5) and free-fed (n=5) and diet-restricted (n=5) DKO mice at 24 weeks. C, Ejection fraction of C57BL6 control mice (n=13) and free-fed (n=12) and diet-restricted (n=12) DKO mice at 24 weeks. †$P<0.05$ vs day values; *$P<0.05$; **$P<0.01$.

these alterations were corrected in diet-restricted DKO mice (Figure 6B).

HR at the time of fractional area change measurements was comparable in C57BL6 mice and in free-fed and diet-restricted DKO mice (406±57 bpm, 433±78 bpm and 377±57 bpm respectively). Ejection fraction of C57BL6 mice was 51±6.2%. At 24 weeks, ejection fraction of DKO mice was significantly lower (38±7.1%; $P<0.01$). Diet restriction restored ejection fraction to 50±5.5 ($P<0.001$) (Figure 6C).

Discussion

In this study, we demonstrated lower PPAR-α and PPAR-γ expression in obese, insulin-resistant mice compared with lean mice. Diet restriction resulted in an upregulation of both PPAR-α and PPAR-γ in the adipose tissue, the heart, and the aortic arch. Increased PPAR expression in the adipose tissue of diet-restricted mice was related to an increased expression of genes that explain increased glucose transport and insulin sensitivity, reduced hypertriglyceridemia, reduced oxidative stress and inflammation, improved cardiovascular function, and reduced atherosclerosis on weight loss. The inverse relation between PPAR-α and PPAR-γ expression and the aortic plaque volume in general and the accumulation of ox-LDL in particular in those mice support the hypothesis that PPAR regulation is a key mechanism in the weight loss–associated inhibition of atherosclerosis. Weight reduction in DKO mice that had extensive atherosclerosis at the time of diet restriction resulted not only in an inhibition of further plaque progression but also in a decrease of the macrophage content and an increase of the smooth muscle cell content, suggesting stabilization of plaques. All these changes were observed in the absence of leptin. Although weight loss was associated with a decrease in triglycerides, there was no effect on total cholesterol.

Glucose Transport and Insulin Sensitivity

Ligands of PPAR-γ stimulate adipocyte differentiation, which is associated with alleviation of insulin resistance, presumably because of decreases in free fatty acids and upregulation of adiponectin.[21] They also improve glucose uptake in insulin-resistant tissues via an increase in the glucose transporter GLUT-4.[22,23] Analysis of gene expression of adipocytes of insulin-resistant patients showed a decreased expression of PPAR-γ, adiponectin, fatty acid–binding protein (FABP), and LPL.[24–26] Insulin-stimulated activation of MEK/ERK signaling promoted adipogenesis by enhancing C/EBP-α and PPAR-γ gene expression in vitro.[27] Insulin-stimulated PPAR-γ expression depends on the prenylation of the Ras family GTPases, which ensure normal phosphorylation and activation of CREB, which, in turn, triggers the intrinsic cascade of adipogenesis by inducing the expression of GLUT-4.[28] Here, the increased PPAR gene expression was associated with increased gene expression of Ras, GLUT-4, FABP, C/EBPα, and LPL. Plasma concentrations of adiponectin were higher in diet-restricted than in free-fed DKO mice, which is in agreement with the finding in humans that plasma adiponectin predicts insulin sensitivity of both glucose and lipid metabolism.[29] Taken together, all these changes explain the increase in insulin sensitivity on weight loss.

Correction of Hypertriglyceridemia

Reduction of triglycerides in diet-restricted DKO mice can be explained by increased expression of PPAR-α, lipoprotein lipase (LPL), the hormone-sensitive lipase, and the VLDL receptor. On severe fasting, PPAR-α activity and expression are induced in rodents, allowing the catabolism of fatty acids to produce ketone bodies, which serve as energy sources for extrahepatic tissues. In humans, pharmacological PPAR-α activation with fibrates decreases plasma triglycerides by increasing fatty acid uptake and catabolism, resulting in limited triglyceride and VLDL production by the liver.[30] LPL catalyzes the hydrolysis of triglycerides[31] and modulates the binding of triglyceride-rich VLDL particles to the VLDL receptor.[32] Conversely, LPL-induced lipolysis of triglyceride-rich lipoproteins generates PPAR-α ligands, providing a link between lipoprotein metabolism and distal PPAR transcriptional effects.[33] Lipid metabolism plays an important role in glucose homeostasis. A reduction in circulating or intracellular lipids by activation of PPAR-α improved insulin sensitivity and the diabetic condition of mice.[34] In adipocytes, skeletal muscle, and pancreatic β-cells, lipids are mobilized by the hormone-sensitive lipase, which deficiency results in a moderate impairment of insulin sensitivity.[35]

Oxidative Stress, Inflammation, and Reduced Atherosclerosis

Oxidative stress is a key factor in atherogenesis.[36] We have shown increased LDL oxidation in free-fed DKO mice,[5] in agreement with increased circulating ox-LDL in obese persons without clinical evidence of cardiovascular disease.[37,38] Here, we show that weight loss results in reduced oxidation of LDL that can be attributed to increased HDL-associated PON[39] and to increased LCAT activity.[5] Weight loss also resulted in lower expression of arachidonate-5-lipoxygenase, which generates oxidized fatty acids in LDL that are mediators of CHD.[40] Moreover, it resulted in increased expression of superoxide dismutase and of glutathione peroxidase. Decreased activity of these enzymes was associated with increased atherosclerosis.[41] Finally, scavenger-receptor–mediated uptake of ox-LDL by macrophages results in foam cell formation. Platelet factor 4 enhances the uptake of ox-LDL by macrophages.[42] Thus, decreased expression of platelet factor 4 can result in decreased uptake of ox-LDL and thus decreased foam cell generation. The amount of ox-LDL in the aortic arch from diet-restricted DKO mice was indeed lower than that in free-fed mice.

A possible explanation for the negative correlation between both PPAR-α and PPAR-γ expression and the accumulation of ox-LDL in the plaque is that PPAR induction results in improved insulin signaling in macrophages and reduced oxidation of LDL and foam cell formation. This hypothesis is also supported by the recent finding that defective macrophage insulin signaling predisposes to foam cell formation and atherosclerosis in insulin-resistant states and that this is reversed in vivo in DKO mice by treatment with PPAR-γ activators, resulting in increased insulin sensitivity, which is associated with decreased CD36 scavenger-receptor expression in macrophages and thereby decreased deposition of ox-LDL in the plaque.[43] The inverse relation between increased insulin sensitivity as a result of increased PPAR expression and oxidation of LDL

would further strengthen the validity of this model for studying cardiovascular disease mechanisms associated with the metabolic syndrome. Indeed, we have recently shown that the metabolic syndrome in humans is associated with elevated circulating ox-LDL, which predicts the risk for future myocardial infarction.[44]

Inflammation plays an important role in atherosclerosis.[45] Adipocytes also contribute to these processes.[45,46] PPAR agonists may not only regulate metabolic processes but also limit inflammatory responses, including some involved in atherosclerosis.[47,48] Indeed, PPAR-γ activators inhibit the expression of intercellular adhesion molecule-1 in activated endothelial cells and reduce monocyte/macrophage homing to atherosclerotic plaques.[49] We identified increased intercellular adhesion molecule-1 expression and macrophage homing as an important mechanism of increased atherosclerosis in DKO mice.[5] PPAR-γ also suppresses thromboxane synthase gene expression, which also could contribute to the reduction in hypertension.[50] Furthermore, the expression of CD22, CD44, CD53, and CD68 was decreased in diet-restricted DKO mice. The latter is particularly interesting because overexpression of the receptor for advanced glycation end products in diabetic $CD68^+$ macrophages is associated with enhanced inflammatory reaction. Expression of mast cell proteases, which degrade HDL-associated apolipoproteins and thereby reduce their ability to promote cellular cholesterol efflux,[51] was also decreased.

Cardiovascular Function

Our analysis of circadian variation of BP and HR in unrestrained mice, reflecting autonomic control, showed an elevated SBP, DBP, and HR in free-fed DKO mice and the absence of a physiological "dip" of BP and HR during the resting (daylight) period. Both anomalies recapitulate similar observations in human obesity-associated hypertension and are more generally associated with defects of the parasympathetic and/or sympathetic components of the arterial baroreflex.[52]

To gain more understanding in the underlying defective control mechanism, we performed spectral analysis of BP and HR variability in the frequency domain. The observed sympathovagal imbalance, with increased SBP variability in the low frequencies, reflects increased orthosympathetic activity. The decreased variability of HR in the HF domain reflects impaired activity of the parasympathetic nervous system. This is further confirmed by the higher basal HR in free-fed DKO mice. The increased variability of SBP in the VLF domain points to mixed effects of neurohumoral control mechanisms of BP and the short-term buffering effect of NO on BP.[53] Indeed, a similar higher BP variability in the VLF band is distinctively observed in mice genetically deficient in endothelial NOS that are also hypertensive.[19] We and others have shown that the NOS pathway is a major "buffering" system of systolic BP and that chronic dyslipidemia specifically alters endothelial NO synthesis, with a resultant increased variability of SBP.[18,19]

An important observation in our study is that diet restriction and weight loss normalized BP, restored BP circadian variation, and normalized BP and HR variability in the VLF, LF, and HF bands, respectively (Figure 6). The increased variability of BP in free-fed DKO mice and the decrease of this variability on weight loss are potentially clinically important observations, given the adverse prognosis associated with increased SBP variability in humans.[54] Our observation of *NOS3* upregulation after diet restriction in adipocyte tissue, if reflective of similar changes in the peripheral vasculature, would provide a strong mechanistic explanation for the restoration of endothelium and NOS-dependent BP regulation and vagal control of HR. We also observed increased expression of angiotensinogen in adipose tissue from diet-restricted mice. A local renin-angiotensinogen system in adipose tissue gives rise to angiotensin II, which stimulates the production of prostacyclin, which, acting as an adipogenic hormone, promotes the differentiation of preadipocytes into adipocytes by activating all PPAR isoforms, and acting as a vasodilator, can reduce hypertension.[55,56]

Conclusions

Inhibition of atherosclerosis and improvement of cardiovascular function after weight loss in leptin-deficient, obese, and insulin-resistant mice can be explained by expressional changes of key genes regulating oxidative stress, lipid metabolism, and endothelial function, most of which are under the transcriptional control of PPARs. Our observation of restored/increased expression of PPARs in the same condition and the correlation between PPAR expression and plaque volume in DKO mice points to the critical role of these transcription factors in both the pathogenesis and the potential treatment of these features of the metabolic syndrome.

Acknowledgments

This study was supported in part by the Fonds voor Wetenschappelijk Onderzoek–Vlaanderen (Program G027604) and the Interuniversity Attraction Poles Program, Belgian Science Policy (P5/02). We thank Hilde Bernar, Els Deridder, Michèle Landeloos, and Dominique Stengel (INSERM U525) for excellent technical assistance.

References

1. Haffner SM, Mykkanen L, Festa A, et al. Insulin-resistant prediabetic subjects have more atherogenic risk factors than insulin-sensitive prediabetic subjects: implications for preventing coronary heart disease during the prediabetic state. *Circulation*. 2000;101:975–980.
2. Abate N, Garg A, Peshock RM, et al. Relationships of generalized and regional adiposity to insulin sensitivity in men. *J Clin Invest*. 1995;96:88–98.
3. McLaughlin T, Abbasi F, Kim HS, et al. Relationship between insulin resistance, weight loss, and coronary heart disease risk in healthy, obese women. *Metabolism*. 2001;50:795–800.
4. Henkin L, Bergman RN, Bowden DW, et al. Genetic epidemiology of insulin resistance and visceral adiposity: the IRAS Family Study design and methods. *Ann Epidemiol*. 2003;13:211–217.
5. Mertens A, Verhamme P, Bielicki JK, et al. Increased low-density lipoprotein oxidation and impaired high-density lipoprotein antioxidant defense are associated with increased macrophage homing and atherosclerosis in dyslipidemic obese mice: LCAT gene transfer decreases atherosclerosis. *Circulation*. 2003;107:1640–1646.
6. Hasty AH, Shimano H, Osuga J, et al. Severe hypercholesterolemia, hypertriglyceridemia, and atherosclerosis in mice lacking both leptin and the low density lipoprotein receptor. *J Biol Chem*. 2001;276:37402–37408.
7. Nagy TR, Clair AL. Precision and accuracy of dual-energy X-ray absorptiometry for determining in vivo body composition of mice. *Obes Res*. 2000;8:392–398.
8. Van Eck M, Twisk J, Hoekstra M, et al. Differential effects of scavenger receptor BI deficiency on lipid metabolism in cells of the arterial wall and in the liver. *J Biol Chem*. 2003;278:23699–23705.
9. Yang YH, Dudoit S, Luu P, et al. Normalization for cDNA microarray data: a robust composite method addressing single and multiple slide systematic variation. *Nucleic Acids Res*. 2002;30:e15.
10. Hedrick CC, Castellani LW, Warden CH, et al. Influence of mouse apolipoprotein A-II on plasma lipoproteins in transgenic mice. *J Biol Chem*. 1993;268:20676–20682.

11. Vercaemst R, Rosseneu M, Van Biervliet JP. Separation and quantitation of plasma lipoproteins by high-performance liquid chromatography. *J Chromatogr*. 1983;276:174–181.
12. Ludwig DS, Tritos NA, Mastaitis JW, et al. Melanin-concentrating hormone overexpression in transgenic mice leads to obesity and insulin resistance. *J Clin Invest*. 2001;107:379–386.
13. Bielicki JK, Forte TM. Evidence that lipid hydroperoxides inhibit plasma lecithin:cholesterol acyltransferase activity. *J Lipid Res*. 1999;40: 948–954.
14. Blankenberg S, Stengel D, Rupprecht HJ, et al. Plasma PAF-acetylhydrolase in patients with coronary artery disease: results of a cross-sectional analysis. *J Lipid Res*. 2003;44:1381–1386.
15. Mackness MI, Arrol S, Abbott C, et al. Protection of low-density lipoprotein against oxidative modification by high-density lipoprotein associated paraoxonase. *Atherosclerosis*. 1993;104:129–135.
16. Butz GM, Davisson RL. Long-term telemetric measurement of cardiovascular parameters in awake mice: a physiological genomics tool. *Physiol Genomics*. 2001;5:89–97.
17. Just A, Faulhaber J, Ehmke H. Autonomic cardiovascular control in conscious mice. *Am J Physiol*. 2000;279:R2214–R2221.
18. Pelat M, Dessy C, Massion P, et al. Rosuvastatin decreases caveolin-1 and improves nitric oxide-dependent heart rate and blood pressure variability in apolipoprotein $E^{-/-}$ mice in vivo. *Circulation*. 2003;107: 2480–2486.
19. Stauss HM, Godecke A, Mrowka R, et al. Enhanced blood pressure variability in eNOS knockout mice. *Hypertension*. 1999;33:1359–1363.
20. Yang XP, Liu YH, Rhaleb NE, et al. Echocardiographic assessment of cardiac function in conscious and anesthetized mice. *Am J Physiol*. 1999;277:H1967–H1974.
21. Yamauchi T, Kamon J, Waki H, et al. The mechanisms by which both heterozygous peroxisome proliferator-activated receptor gamma (PPARgamma) deficiency and PPARgamma agonist improve insulin resistance. *J Biol Chem*. 2001;276:41245–41254.
22. Komers R, Vrana A. Thiazolidinediones: tools for the research of metabolic syndrome X. *Physiol Res*. 1998;47:215–225.
23. Young PW, Cawthorne MA, Coyle PJ, et al. Repeat treatment of obese mice with BRL 49653, a new potent insulin sensitizer, enhances insulin action in white adipocytes: association with increased insulin binding and cell-surface GLUT4 as measured by photoaffinity labeling. *Diabetes*. 1995;44:1087–1092.
24. Hensley LL, Ranganathan G, Wagner EM, et al. Transgenic mice expressing lipoprotein lipase in adipose tissue: absence of the proximal 3′-untranslated region causes translational upregulation. *J Biol Chem*. 2003;278:32702–32709.
25. Hong G, Davis B, Khatoon N, et al. PPAR gamma-dependent anti-inflammatory action of rosiglitazone in human monocytes: suppression of TNF alpha secretion is not mediated by PTEN regulation. *Biochem Biophys Res Commun*. 2003;303:782–787.
26. Jansson PA, Pellme F, Hammarstedt A, et al. A novel cellular marker of insulin resistance and early atherosclerosis in humans is related to impaired fat cell differentiation and low adiponectin. *FASEB J*. 2003;17: 1434–1440.
27. Prusty D, Park BH, Davis KE, et al. Activation of MEK/ERK signaling promotes adipogenesis by enhancing peroxisome proliferator-activated receptor gamma (PPARgamma) and C/EBPalpha gene expression during the differentiation of 3T3-L1 preadipocytes. *J Biol Chem*. 2002;277: 46226–46232.
28. Klemm DJ, Leitner JW, Watson P, et al. Insulin-induced adipocyte differentiation: activation of CREB rescues adipogenesis from the arrest caused by inhibition of prenylation. *J Biol Chem*. 2001;276:28430–28435.
29. Tschritter O, Fritsche A, Thamer C, et al. Plasma adiponectin concentrations predict insulin sensitivity of both glucose and lipid metabolism. *Diabetes*. 2003;52:239–243.
30. Barbier O, Torra IP, Duguay Y, et al. Pleiotropic actions of peroxisome proliferator-activated receptors in lipid metabolism and atherosclerosis. *Arterioscler Thromb Vasc Biol*. 2002;22:717–726.
31. Mead JR, Ramji DP. The pivotal role of lipoprotein lipase in atherosclerosis. *Cardiovasc Res*. 2002;55:261–269.
32. Takahashi S, Sakai J, Fujino T, et al. The very low density lipoprotein (VLDL) receptor: a peripheral lipoprotein receptor for remnant lipoproteins into fatty acid active tissues. *Mol Cell Biochem*. 2003;248: 121–127.
33. Ziouzenkova O, Perrey S, Asatryan L, et al. Lipolysis of triglyceride-rich lipoproteins generates PPAR ligands: evidence for an antiinflammatory role for lipoprotein lipase. *Proc Natl Acad Sci U S A*. 2003;100: 2730–2735.
34. Kim H, Haluzik M, Asghar Z, et al. Peroxisome proliferator-activated receptor-alpha agonist treatment in a transgenic model of type 2 diabetes reverses the lipotoxic state and improves glucose homeostasis. *Diabetes*. 2003;52:1770–1778.
35. Mulder H, Sorhede-Winzell M, Contreras JA, et al. Hormone-sensitive lipase null mice exhibit signs of impaired insulin sensitivity whereas insulin secretion is intact. *J Biol Chem*. 2003;278:36380–36388.
36. Mertens A, Holvoet P. Oxidized LDL and HDL: antagonists in atherothrombosis. *FASEB J*. 2001;15:2073–2084.
37. Holvoet P, Mertens A, Verhamme P, et al. Circulating oxidized LDL is a useful marker for identifying patients with coronary artery disease. *Arterioscler Thromb Vasc Biol*. 2001;21:844–848.
38. Holvoet P, Harris TB, Tracy RP, et al. Association of high coronary heart disease risk status with circulating oxidized LDL in the well-functioning elderly: findings from the Health, Aging, and Body Composition Study. *Arterioscler Thromb Vasc Biol*. 2003;23:1444–1448.
39. Mackness B, Durrington P, McElduff P, et al. Low paraoxonase activity predicts coronary events in the Caerphilly Prospective Study. *Circulation*. 2003;107:2775–2779.
40. Navab M, Berliner JA, Subbanagounder G, et al. HDL and the inflammatory response induced by LDL-derived oxidized phospholipids. *Arterioscler Thromb Vasc Biol*. 2001;21:481–488.
41. 't Hoen PA, Van der Lans CA, Van Eck M, et al. Aorta of apoE-deficient mice responds to atherogenic stimuli by a prelesional increase and subsequent decrease in the expression of antioxidant enzymes. *Circ Res*. 2003;93:262–269.
42. Nassar T, Sachais BS, Akkawi S, et al. Platelet factor 4 enhances the binding of oxidized low-density lipoprotein to vascular wall cells. *J Biol Chem*. 2003;278:6187–6193.
43. Liang CP, Han S, Okamoto H, et al. Increased CD36 protein as a response to defective insulin signaling in macrophages. *J Clin Invest*. 2004;113: 764–773.
44. Holvoet P, Kritchevsky SB, Tracy RP, et al. The metabolic syndrome, circulating oxidized LDL, and risk of myocardial infarction in well-functioning elderly people in the health, aging, and body composition cohort. *Diabetes*. 2004;53:1068–1073.
45. Libby P. Inflammation in atherosclerosis. *Nature*. 2002;420:868–874.
46. Rajala MW, Scherer PE. Minireview: the adipocyte: at the crossroads of energy homeostasis, inflammation, and atherosclerosis. *Endocrinology*. 2003;144:3765–3773.
47. Hsueh WA, Law R. The central role of fat and effect of peroxisome proliferator-activated receptor-gamma on progression of insulin resistance and cardiovascular disease. *Am J Cardiol*. 2003;92:3J–9J.
48. Plutzky J. The potential role of peroxisome proliferator-activated receptors on inflammation in type 2 diabetes mellitus and atherosclerosis. *Am J Cardiol*. 2003;92:34J–41J.
49. Pasceri V, Wu HD, Willerson JT, et al. Modulation of vascular inflammation in vitro and in vivo by peroxisome proliferator-activated receptor-γ activators. *Circulation*. 2000;101:235–238.
50. Ikeda Y, Sugawara A, Taniyama Y, et al. Suppression of rat thromboxane synthase gene transcription by peroxisome proliferator-activated receptor gamma in macrophages via an interaction with NRF2. *J Biol Chem*. 2000;275:33142–33150.
51. Lee M, Sommerhoff CP, von Eckardstein A, et al. Mast cell tryptase degrades HDL and blocks its function as an acceptor of cellular cholesterol. *Arterioscler Thromb Vasc Biol*. 2002;22:2086–2091.
52. Makino M, Hayashi H, Takezawa H, et al. Circadian rhythms of cardiovascular functions are modulated by the baroreflex and the autonomic nervous system in the rat. *Circulation*. 1997;96:1667–1674.
53. Stauss HM, Persson PB. Role of nitric oxide in buffering short-term blood pressure fluctuations. *News Physiol Sci*. 2000;15:229–233.
54. Sega R, Corrao G, Bombelli M, et al. Blood pressure variability and organ damage in a general population: results from the PAMELA study (Pressioni Arteriose Monitorate E Loro Associazioni). *Hypertension*. 2002;39:710–714.
55. Ailhaud G. Cross talk between adipocytes and their precursors: relationships with adipose tissue development and blood pressure. *Ann N Y Acad Sci*. 1999;892:127–133.
56. Engeli S, Schling P, Gorzelniak K, et al. The adipose-tissue renin-angiotensin-aldosterone system: role in the metabolic syndrome? *Int J Biochem Cell Biol*. 2003;35:807–825.